Advanced design and optimization of wind turbines based on turbine theories

Zh Zhang

Zurch University of Applied Science, Zurich, Switzerland
E-mail: zhengji.zhang@zhaw.ch

Abstract. A review of wind turbine technology showed that many flaws in both the flow models and computations are involved in the traditional fundamentals. While traditional methods for design and computation are all based on the airfoil theory, a new method based on turbine theories has been developed and is shown to be ideally applicable. Against the traditional method, the new method also considers non-uniform pressure distribution in flows downstream of the rotor plane and is thus highly accurate. The blade efficiency or tip swirl number has been introduced. It enables computation of the power coefficient to be very reasonable. Its optimum can be directly applied to the geometrical design of turbine blades. Between the tip speed ratio λ, blade efficiency ε, and power coefficient c_p, a closed solution of both the optimum design and the operation of wind turbines exists. It is demonstrated that the maximum achievable power coefficient can be 10% larger than that predicted by all previous theories.

1. Introduction

In times of increased use of renewable energies, wind energy is gaining increased attention. More and more wind turbines are installed both on-shore and off-shore. Modern manufacture technology enables large wind turbines with a power output up to 8 MW to be built and installed.

Wind power technology basically comprises flow-dynamic design, manufactures and operations of wind turbines. The fundamental technology of wind turbines is thus fluid mechanics and aerodynamics. First, Betz's law, based on flow dynamics, limits the maximum achievable power at 59% (power coefficient c_p=0.59). Second, aerodynamic designs of wind turbines are uniquely based on airfoil theory, to which apply the Schmitz theory and the blade element momentum method (BEM) [1, 2].

A review of these fundamentals demonstrates that, first, all these basics are insufficient if compared with those in water turbines. Second, as indicated in this paper, they are to some extent imperfect or inaccurate and could lead to significant design errors. Third, the reachable efficiencies of wind turbines (<75% of Betz's maximum) are generally much lower than those in water turbines (>90%). For the most fundamental Betz law, for instance, only the flow through the "actuator disc" is considered for balancing the pressure forces and the resistance force based on the momentum equation. A detailed study by the author of this paper showed that the used actuator-disc model is not exact. The Schmitz theory and the BEM suppose that the flow through the turbine wheel is comparable to the flow passing through a single blade as treated by the airfoil theory. Because it is in reality not the same and the non-uniform pressure distribution in the flow has been ignored, one has to make corrections in the aerodynamic design of the blade profiles. In other words, both the Schmitz theory and the BEM have followed considerable detours with unreasonable assumptions in computing and designing the blade profiles.

Some defects in fundamentals of wind turbines will be indicated below in Sect. 2. They are found in both Betz's law and Schmitz's theory including the BEM for turbine design.
Primarily, this paper aims to introduce a new design method of turbine wheels based on much effective turbine theories (instead of the airfoil theory). At its center is the application of the Euler equation for specific work in fluid machinery. For this reason, it is indispensible to reveal the most significant flow dynamic fundamentals of wind turbines and to present conditions for applying the Euler equation.

2. Defects in fundamentals of wind turbine technology

The fundamental background of wind turbine technology is the Betz law which is derived based on the Froude-Rankine theorem. The flow through an "actuator disc" is considered according to figure 1. There, in a 2D-view, the control volume for mass and momentum conservations is bounded by two streamlines which pass through die edge of the disc. At section 3, the flow velocity has the value c_3 and the pressure reaches the ambient pressure p_0. The flow resistance (thrust) caused by the disc is denoted by T. It is computed for steady flow by applying the momentum law to the volume flow Q from section 0 to section 3:

$$T = \rho\dot{Q}(c_0 - c_3) \tag{1}$$

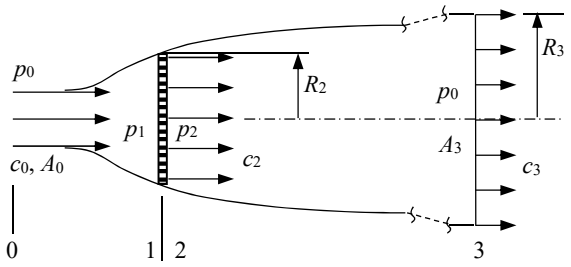

Figure 1. Actuator disc and flows.

Based on the mechanical principle, use of the momentum law to determine the flow resistance requires that a control volume around a disc must be given by real streamlines. This condition is obviously not fulfilled in figure 1. Because of the singularity at the edge of the disc and thus the flow separation there, the streamlines shown in figure 1 will no longer maintain after the disc. The flow model shown in figure 1 must be considered as the first flaw or defect in the fundamentals of wind power technology. As will be shown below, many disagreements and faults found in analyses are connected to this flaw.
On the other hand, the thrust is computed with the resistance coefficient c_D as

$$T = c_D A_D \frac{1}{2}\rho c_0^2 \tag{2}$$

with A_D as the physical area of the disc.
Equalizing Eq. (1) and (2) with $\dot{Q} = c_0 A_0$ and $c_3 A_3 = c_0 A_0$ yields

$$c_D = 2\frac{A_0}{A_D}\left(1 - \frac{A_0}{A_3}\right) \tag{3}$$

The power which is related to the thrust on the disc is computed as $P=c_2T$. Because of Eq. (1), this is written as

$$P = \rho\dot{Q}c_2(c_0 - c_3) \tag{4}$$

Moreover, with $p_3=p_0$ at section 3, the power extracted from the air flow between section 0 and 3 can be expressed as

$$P = \frac{1}{2}\rho\dot{Q}\left(c_0^2 - c_3^2\right) \tag{5}$$

Equalizing Eq. (4) and (5) yields

$$c_2 = \frac{1}{2}\left(c_0 + c_3\right) \tag{6}$$

This relation is known as the Froude-Rankine theorem. Because the mean velocity c_2 is used in association with $P=c_2T$, it is in fact not proved to be applicable to computations of the volume flow rate by multiplying the area of the actuator disc. In all previous applications, the difference has been simply ignored. This must be considered as the second flaw or defect in the fundamentals of wind power technology.

By assuming the velocity c_2 to be equal to that for volume flow, the volume flow rate through the actuator disc is given as $\dot{Q} = c_2 A_\mathrm{D}$. Then, it follows from Eq. (6) with $c_0 A_0 = c_2 A_\mathrm{D} = c_3 A_3$

$$\frac{A_0}{A_\mathrm{D}} = \frac{1}{2}\left(1 + \frac{A_0}{A_3}\right) \tag{7}$$

Combining this equation with Eq. (3) yields

$$\frac{A_0}{A_3} = \sqrt{1 - c_\mathrm{D}} \tag{8}$$

For a closed disc (A_0=0), it follows c_D=1. This resistance coefficient does not exactly agree with measurements leading to c_D=1.1 to 1.17. The reason for this disagreement lies obviously in both the first and the second flaws mentioned above.

The power coefficient of the actuator disc is defined by relating the extracted power to the total power of air flow through a flow area equal to the disc area. With $\dot{Q} = c_0 A_0$ one obtains

$$c_\mathrm{p} = \frac{P}{\frac{1}{2}\rho c_0^2 A_\mathrm{D} c_0} = \frac{A_0}{A_\mathrm{D}}\left(1 - \frac{c_3^2}{c_0^2}\right) = \frac{A_0}{A_\mathrm{D}}\left(1 - \frac{A_0^2}{A_3^2}\right) \tag{9}$$

Because of Eq. (7), this is further written as

$$c_\mathrm{p} = \frac{1}{2}\left(1 + \frac{A_0}{A_3}\right)\left(1 - \frac{A_0^2}{A_3^2}\right) \tag{10}$$

This is the Betz law. The power coefficient is expressed as a function of the area ratio A_0/A_3. It is easy to show that the maximum power coefficient is given at A_0/A_3=1/3, at which one obtains

$$c_\mathrm{p,max} = \frac{16}{27} = 0.593 \tag{11}$$

This is the Betz limit of maximum extractable energy from the air flow.

At the closed disc (A_0=0), the power coefficient does not vanish but takes c_p=0.5. This value is obviously incorrect. The reasons are again the first and the second flaws in the fundamentals of wind power technology, as mentioned above.

Physically, the meaning of the area ratio A_0/A_3=1/3 is unclear. Especially, it is not clear, how it is related to flow dynamic property of the used actuator disc. For this reason, A_0/A_3 from Eq. (8) is further concerned and inserted into Eq. (10). One obtains

$$c_\mathrm{p} = \frac{1}{2}c_\mathrm{D}\left(1 + \sqrt{1 - c_\mathrm{D}}\right) \tag{12}$$

This novel equation with independent variable c_D is obviously much more meaningful than Eq. (10) with independent variable A_0/A_3, which appears to be incomprehensible because of the flow area A_3.

The corresponding maximum of the power coefficient is found at an actuator disc with $c_{D,m}$=8/9. Figure 2 shows the graph of Eq. (12).
As indicated above, two flaws in the fundamentals of wind power technology have been confirmed. Extended studies with corresponding improvements have been conducted by the author of this paper. One of them is based on a new flow model with streamlines away from the actuator disc, different from that in figure 1. For comparison, the first approach of new computations has also been shown in figure 2. The Betz limit has been exceeded by a new limit $c_{p,max}$=0.61, which is predicted at an actuator disc with $c_{D,m}$=1.10 in the closed position. The details of computations will be published soon.

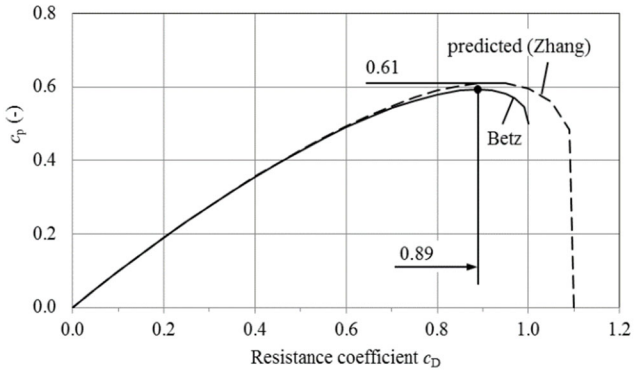

Figure 2. Recalculated Betz law for the power coefficient c_p as a function of the resistance coefficient c_D of an actuator disc.

3. Turbine theory and applications

3.1. Potential flow and flow distribution

The most significant difference between air flows at a wind turbine and a single blade is that the flow after the wind turbine maintains its rotation. This rotation is basically an indication of the extracted power from the air flow. That is to say that it is tightly related to the specific work based on the Euler equation.
The flow before entering the wind turbine is a sort of potential flow. Because viscous friction only has a negligible influence on the flow distributions both in the rotor plane and after the turbine wheel, the flows can be assumed to satisfactorily fulfill the condition of potential flows.

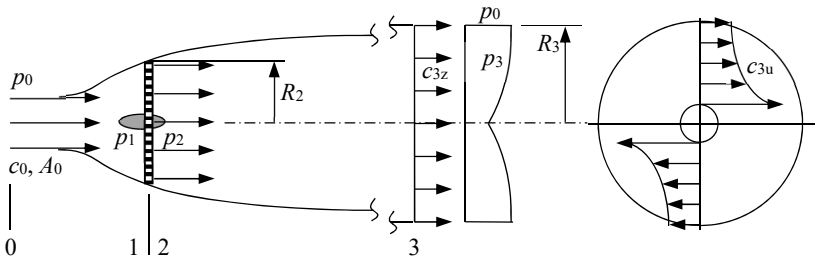

Figure 3. Flow and the flow rotations both at and downstream of a wind turbine wheel.

A new flow model with rotation after the wind turbine is shown in figure 3. For simplicity of the analysis, the control volume of the flow is again assumed to be bounded by axial-flow streamlines which pass through the perimeter of the turbine wheel. The axial velocity component at each flow section is uniform. Because of the rotation, however, both the distribution of the circumferential velocity component and the pressure distribution are non-uniform. In section 2, the rotation of fluid (velocity component c_{2u}) must fulfill the condition of potential flows and is thus characterized as

$$c_{2u} r_2 = c_{2u,R} R_2 = \text{const} \tag{13}$$

or because of $u_2=r_2\omega$, with ω as the angular rotational speed,

$$u_2 c_{2u} = u_{2,R} c_{2u,R} = \text{const} \tag{14}$$

On the other hand, the pressure distribution in section 2 is determined, from Euler equations (fluid dynamics), by

$$\frac{\partial p_2}{\partial r_2} = \rho \frac{c_{2u}^2}{r_2} \tag{15}$$

With respect to Eq. (13) satisfying the potential flow condition as given by $c_{2u} = (R_2/r_2)c_{2u,R}$, one obtains by integrating the above equation the pressure distribution

$$p_2 + \frac{1}{2}\rho c_{2u}^2 = p_{2,R} + \frac{1}{2}\rho c_{2u,R}^2 \tag{16}$$

This is a type of energy equation. It states that along the radial coordinate in section 2 the energy is constant and equal to that on the boundary at the radius R_2. In fact, such a flow distribution exactly agrees with the condition for assumed potential flow, i.e., the total pressure is constant.
Both $p_{2,R}$ and $c_{2u,R}$ in the above equation need to be determined. The flow from section 2 towards section 3 must fulfill the condition of potential flow and the law of conservation of angular momentum. This means, for instance, that along the boundary streamlines there must be $c_{3u,R}R_3 = c_{2u,R}R_2$ for the velocity component c_u. In section 3, the rotation of the flow is characterized in a similar way as

$$u_3 c_{3u} = u_{3,R} c_{3u,R} = \text{const} \tag{17}$$

Correspondingly, like Eq. (16), there is (with $p_{3,R}=p_0$)

$$p_3 + \frac{1}{2}\rho c_{3u}^2 = p_0 + \frac{1}{2}\rho c_{3u,R}^2 \tag{18}$$

To determine the parameter $p_{2,R}$ of Eq. (16), the energy balance between section 2 and 3 is considered. According to the Bernoulli equation, it follows

$$p_{2,R} + \frac{1}{2}\rho\left(c_{2u,R}^2 + c_{2x}^2\right) = p_0 + \frac{1}{2}\rho\left(c_{3u,R}^2 + c_{3x}^2\right) \tag{19}$$

In explicit form, this is also written as

$$p_{2,R} = p_0 - \frac{1}{2}\rho c_{2u,R}^2\left(1 - \frac{c_{3u,R}^2}{c_{2u,R}^2}\right) - \frac{1}{2}\rho c_{2x}^2\left(1 - \frac{c_{3x}^2}{c_{2x}^2}\right) \tag{20}$$

Then, employing $c_{3u,R}R_3 = c_{2u,R}R_2$ and $c_{3x}A_3 = c_{2x}A_2$, one further obtains

$$p_{2,R} = p_0 - \frac{1}{2}\rho\left[c_{2u,R}^2 + c_{2x}^2\left(1 + \frac{A_2}{A_3}\right)\right]\left(1 - \frac{A_2}{A_3}\right) \tag{21}$$

The parameter $c_{2u,R}$ will be determined in the next section in connection with the Euler equation for specific work.

3.2. Euler equation and specific work with uniform distribution

To determine the power exchange between the wind flow and the turbine wheel, the flow in section 2, i.e., after the rotor plane is considered. According to the Euler equation and in view of Eq. (14), the specific work exchanged between the flow and the wind turbine is given by

$$Y = u_2 c_{2u} = u_{2,R} c_{2u,R} = \text{const} \tag{22}$$

This is a very pleasing fact. Along the radial coordinate, constant specific work is obtained. This uniform energy extraction just represents an ideal case which should be approached for each blade design. With the total volume flow rate, the total power exchange between the flow and the wind turbine is then given as

$$P = \rho \dot{Q} u_{2,\mathrm{R}} c_{2\mathrm{u,R}} \tag{23}$$

On the other hand, the power extracted from the wind flow is obtained from the energy balance between section 0 and 3. To this end, first, the total pressure in the flow at section 3 is given by

$$p_{3,\mathrm{tot}} = p_3 + \frac{1}{2}\rho\left(c_{3\mathrm{x}}^2 + c_{3\mathrm{u}}^2\right) \tag{24}$$

Because of Eq. (18), this is further written as

$$p_{3,\mathrm{tot}} = p_0 + \frac{1}{2}\rho\left(c_{3\mathrm{u,R}}^2 + c_{3\mathrm{x}}^2\right) \tag{25}$$

Then, the power extracted from the air flow is obtained as $P = \dot{Q}\left(p_{0,\mathrm{tot}} - p_{3,\mathrm{tot}}\right)$, which alternatively can also be written as

$$P = \frac{1}{2}\rho\dot{Q}\left(c_0^2 - c_{3\mathrm{x}}^2 - c_{3\mathrm{u,R}}^2\right) \tag{26}$$

Equalizing Eqs. (23) and (26) and using $c_{3\mathrm{u,R}} R_3 = c_{2\mathrm{u,R}} R_2$ yields

$$\frac{R_2^2}{R_3^2} c_{2\mathrm{u,R}}^2 + 2u_{2,\mathrm{R}} c_{2\mathrm{u,R}} - \left(c_0^2 - c_{3\mathrm{x}}^2\right) = 0 \tag{27}$$

This is a quadratic equation for $c_{2\mathrm{u,R}}$. Its solution is given as

$$\frac{c_{2\mathrm{u,R}}}{c_0} = -\frac{R_3^2}{R_2^2}\frac{u_{2,\mathrm{R}}}{c_0} + \frac{R_3^2}{R_2^2}\sqrt{\frac{u_{2,\mathrm{R}}^2}{c_0^2} + \frac{R_2^2}{R_3^2}\left(1 - \frac{c_{3\mathrm{x}}^2}{c_0^2}\right)} \tag{28}$$

In this equation, the velocity ratio $c_{3\mathrm{x}}/c_0$ can be replaced by A_0/A_3; furthermore, $R_2^2/R_3^2 = A_2/A_3$. When, additionally, using the tip speed ratio $\lambda = u_{2,\mathrm{R}}/c_0$ of the turbine wheel, then one obtains

$$\frac{c_{2\mathrm{u,R}}}{c_0} = \frac{A_3}{A_2}\sqrt{\lambda^2 + \frac{A_2}{A_3}\left(1 - \frac{A_0^2}{A_3^2}\right)} - \lambda\frac{A_3}{A_2} \tag{29}$$

In a first approximation, Eq. (7), arising from the Froude-Rankine theorem, can be applied (here $A_\mathrm{D}=A_2$). This is an approximation, because the fluid rotation has not been considered in the Froude-Rankine theorem. It follows then

$$\frac{c_{2\mathrm{u,R}}}{c_0} = \frac{1}{2}\lambda\left(1 + \frac{A_3}{A_0}\right)\left[\sqrt{1 + \frac{2}{\lambda^2}\frac{A_0}{A_3}\left(1 - \frac{A_0}{A_3}\right)} - 1\right] \tag{30}$$

It appears here as a function of both the tip speed ratio λ and the flow area ratio A_0/A_3. For $A_0=0$, one obtains $c_{2\mathrm{u,R},0}/c_0 = 0.5/\lambda$. This is mathematically correct. But physically, it cannot be true. The reason is again the first and the second flaws in the used simplified flow model in figures 1 and 3.

3.3. Blade efficiency and power coefficient

The specific work is determined by Eq. (22). Because it is uniformly distributed in section 2, it can be used as a system parameter. Its ratio to the specific kinetic energy of the air flow is therefore defined as the blade efficiency:

$$\varepsilon = \frac{Y}{c_0^2/2} = \frac{2u_{2,\mathrm{R}}c_{2\mathrm{u,R}}}{c_0^2} \tag{31}$$

Substituting the tip speed ratio $\lambda = u_{2,\mathrm{R}}/c_0$ and Eq. (30) into this expression yields

$$\varepsilon = 2\lambda\frac{c_{2\mathrm{u,R}}}{c_0} = \lambda^2\left(1+\frac{A_3}{A_0}\right)\left[\sqrt{1+\frac{2}{\lambda^2}\frac{A_0}{A_3}\left(1-\frac{A_0}{A_3}\right)}-1\right] \tag{32}$$

For A_0=0 there is ε=1. This incorrectness, just as in Eq. (30), arises from the first and the second flaws in the used simplified flow model. For A_0/A_3=1 there is ε=0, as expected.
With the definition of the blade efficiency, the power extracted from the wind flow can be recalculated from Eq. (23), leading to

$$P = \varepsilon\rho\dot{Q}\frac{c_0^2}{2} \tag{33}$$

Obviously, the blade efficiency ε is a significant parameter which exactly represents the "turbine efficiency" of converting the kinetic energy of the total collected flow into the mechanical energy. However, it is not denoted as "turbine efficiency", because it is only an intermediate parameter and does not include the maximum of the collected air flow and so does not behave as significant as the power coefficient c_p. It, therefore, does not deserve the denotation "turbine efficiency" which sounds even more pompously than "power coefficient". For this reason, it is denoted by ε rather than η. Furthermore, because of Eq. (32) and the proportionality to $c_{2\mathrm{u,R}}/c_0$, the blade efficiency is also called here "tip swirl number". It behaves, like the tip speed ratio, as a design parameter. As shown below in Sect. 4, the blade efficiency ε is actually of geometrical character.
Analogously to Eq. (9) and in view of Eq. (33), the power coefficient is further obtained as

$$c_\mathrm{p} = \frac{2P}{\rho c_0^2 A_2 c_0} = \frac{\dot{Q}}{c_0 A_2}\varepsilon \tag{34}$$

With $\dot{Q} = c_0 A_0$ and $A_2 = A_\mathrm{D}$ from Eq. (7), this last equation takes the form

$$c_\mathrm{p} = \frac{A_0}{A_2}\varepsilon = \frac{1}{2}\left(1+\frac{A_0}{A_3}\right)\varepsilon \tag{35}$$

It represents a function in form c_p=f(ε,λ), because the area ratio A_0/A_3 is, according to Eq. (32), simply a function of same variables.
Against the Betz law in Eq. (10), the power coefficient shown in Eq. (35) is additionally a function of the rotational speed (n) of the wind turbine, which is involved in both parameters (λ and ε). This exactly represents the objective of the present studies.
Figure 4 displays computational results from Eq. (35). The use of the blade efficiency ε as a design parameter is evidently of great significance. It is possible to directly specify ε_m at which the maximum power coefficient is obtained. As shown in Sect. 4 below, the use of ε_m helps to directly design the turbine blade.
For large value of λ, all computations can be simplified. With respect to the expression under the square root in Eq. (32), it follows first

$$\varepsilon \approx 1-\frac{A_0^2}{A_3^2} \tag{36}$$

Then, Eq. (35) becomes

$$c_\mathrm{p} \approx \frac{1}{2}\left(1+\frac{A_0}{A_3}\right)\left(1-\frac{A_0^2}{A_3^2}\right) \tag{37}$$

It is equal to Eq. (10) of the Betz law.

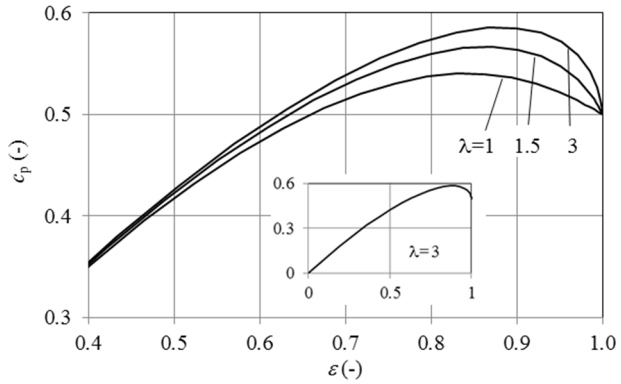

Figure 4. Power coefficient of a wind turbine in dependence on the tip swirl number (ε) for different tip speed ratios (λ).

3.4. Maximum power coefficient and flows

Figure 4 is further considered. Obviously, for each given tip speed ratio λ a tip swirl number ε_m exits, for which the power coefficient assumes its maximum. The function $\varepsilon_m=f(\lambda)$ can be found basically from Eq. (35) together with Eq. (32). An explicit function of $\varepsilon_m=f(\lambda)$, however, cannot be obtained. Based on the analysis, the following two equations can be used for performing iterative computations (with $x=A_0/A_3$):

$$\varepsilon_m = \frac{4x^3}{1-x} + (1-x) \quad \text{and} \quad \frac{\varepsilon_m}{\lambda^2}\frac{x}{1+x} = \sqrt{1+\frac{2}{\lambda^2}x(1-x)} - 1 \tag{38}$$

Computational results are shown in figure 5 by the solid line. It is obtained without any assumption.

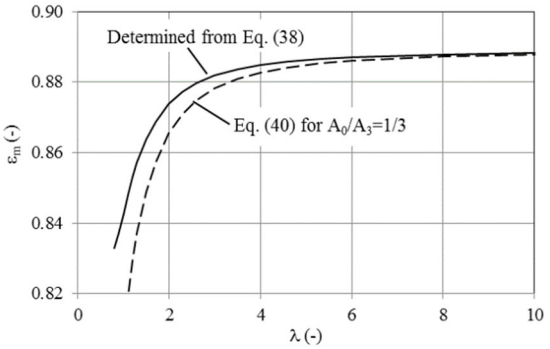

Figure 5. Tip swirl number plotted against the tip speed ratio of the wind turbine under the condition of the maximum power coefficient.

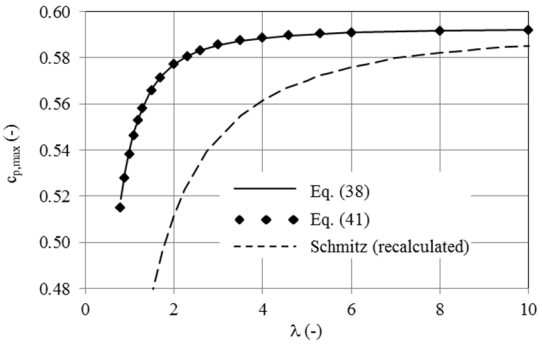

Figure 6. Maximum reachable power coefficient plotted against the tip speed ratio and comparison with computations based on Schmitz's theory.

Once the relation $\varepsilon_m=f(\lambda)$ is obtained, the maximum power coefficient $c_{p,max}=f(\lambda)$ can be computed from Eq. (35) together with Eq. (38), as shown in figure 6 (solid line).

For the case of a large tip speed ratio, one obtains from Eq. (38) the area ratio $(A_0/A_3)_m=1/3$ and further $\varepsilon_m=8/9$. This is comparable with $c_{D,m}=8/9$ in figure 2. The corresponding maximum of the power coefficient is obtained from Eq. (35) as

$$c_{p,max} = \frac{16}{27} \tag{39}$$

It exactly agrees with the Betz limit.

While performing computations for the maximum power coefficient $c_{p,max}$ from Eq. (35), both the area ratio $(A_0/A_3)_m=f(\lambda)$ and the area ratio $(A_0/A_2)_m=f(\lambda)$ have also been found. The former is from Eq. (38) and the latter from Eq. (35), as shown in figure 7. Obviously, only at large tip speed ratios, respective area ratios tend to reach 1/3 and 2/3, which correspond to the condition of Betz's limit for $c_{p,max}$.

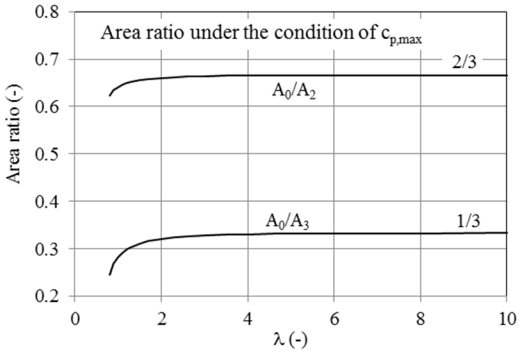

Figure 7. Flow area ratios plotted against the tip speed ratio λ under the condition of maximum reachable power coefficient.

All the above computations have been conducted without any assumptions. They provide a closed solution of ε_m, $c_{p,max}$ and the area ratio A_0/A_2 and A_0/A_3 as a function of only the tip speed ratio λ under the condition of maximum power coefficient. They are therefore applicable for optimum design of the wind turbine.

3.5. Approximations relying on A_0/A_3=1/3

It is known that in Betz's law of using the "actuator disc" model the condition A_0/A_3=1/3 for the maximum power coefficient is applied. If this condition is generally applied in the current case as an approximation, then, one obtains from Eq. (32) and further from Eq. (35), respectively

$$\varepsilon_m \approx 4\lambda^2\left(\sqrt{1+\frac{4}{9\lambda^2}}-1\right) \tag{40}$$

$$c_{p,max} \approx \frac{8}{3}\lambda^2\left(\sqrt{1+\frac{4}{9\lambda^2}}-1\right) \tag{41}$$

For comparison, computations performed with both of these equations have also been shown in figure 5 (dashed line) and figure 6 (symbol), respectively. While in figure 5 good agreement between the two curves is evidenced only at large tip speed ratios, almost exact agreement between Eq. (35), i.e., Eq. (38) and (41) is documented in Figure 6. Thus, Eq. (41) can be considered to be well applicable. Especially, the maximum $c_{p,max}$=16/27 in Eq. (39) can also be directly obtained from Eq. (41) for large tip speed ratio.

The ratio of $c_{p,max}$ to ε_m is 2/3. It also corresponds to the area ratio A_0/A_2 according to Eq. (35).

3.6. About Schmitz's theory and BEM

For the reason of comparison, computations of power coefficients based on Schmitz's theory [1] have also been conducted by the author, as shown in figure 6 (dashed curve). From the literature, curves of computations based on Schmitz's theory are even somewhat lower than those computed here. The Schmitz theory applies in fact also to ideal fluids and was established under all optimum conditions for power exchange, including the Betz condition $A_3=3A_0$. It, however, ignored the non-uniform pressure distribution in the flow. It is, furthermore, based on some assumptions which, unfortunately, even do not fulfill the law of conservation of angular momentum like $c_{3u,R}R_3=c_{2u,R}R_2$ used in the current paper

with Eq. (17). This can be considered as the third flaw or defect in the fundamentals of wind turbine technology.

Against the prediction by Schmitz's theory, the current computations, both Eq. (35) and Eq. (41) based on turbine theories, clearly demonstrate that the maximum reachable power coefficient is significantly higher than believed till now. There is a great reserve and thus possibility to further enhance the power coefficients of wind turbines. At a tip speed ratio λ=2, for instance, the maximum reachable power coefficient can be reset from $c_{p,max}$=0.51 (Schmitz) to $c_{p,max}$=0.57, a difference of more than 10%. For information of readers, in the field of water turbines (Pelton, Francis and Kaplan turbines), engineers have been trying hard since decades to enhance the hydraulic efficiencies of machines only for 1%.

The BEM is actually a computational tool to compute all aerodynamic forces exerted on a given blade and further to compute the aerodynamic performance including the power coefficient of a given wind turbine. It has thus been considered to be only applicable to case studies. Unlike the turbine theories and the Schmitz theory, the BEM is unable to predict the maximum reachable power coefficient in a wind turbine. In addition, the aerodynamic flow at a single airfoil blade fundamentally differs from the aerodynamic flow at a rotating blade, even if it is about a wind wheel with only one blade.

4. Turbine design and operations

The analyses made above can be directly applied to optimize the geometrical design of wind turbines. To this end, the tip swirl number plays a key role. According to figure 5, the tip swirl number is simply a function of tip speed ratio λ. For accurate computations, ε_m and further $c_{2u,R}$ should be computed from Eq. (38) or directly from figure 5. For approximation, however, Eq. (40) can be applied. Together with Eq. (32), it follows

$$\frac{c_{2u,R}}{c_0} = 2\lambda\left(\sqrt{1+\frac{4}{9\lambda^2}}-1\right) \tag{42}$$

It is for the tip radius (R_2) of the blade.

The angular velocity component along the blade in the radial direction is obtained with respect to $c_{2u}r = c_{2u,R}R = \text{const}$ as

$$c_{2u} = 2\lambda c_0\left(\sqrt{1+\frac{4}{9\lambda^2}}-1\right)\frac{R_2}{r} \tag{43}$$

This velocity component represents the flow rotation which must be generated at the turbine wheel.

In the geometrical design of blades, the blade angle (β_b) along the trailing edge of the blade is the most significant parameter. First of all, it must be consistent with the flow angle at the trailing edge of the blade (figure 8) and thus must be designed with respect to the desired velocity component c_{2u}.

According to figure 8 with $u_2=r\omega$ as the circumferential speed of the blade, the following geometrical relation between three velocity vectors can be obtained:

$$c_{2u} + r\omega = w_2\cos\beta_2 \tag{44}$$

With $w_2 = c_{2x}/\sin\beta_2$ this implies

$$\tan\beta_2 = \frac{c_{2x}}{c_{2u}+r\omega} \tag{45}$$

Inserting Eq. (43) and with $\lambda = R_2\omega/c_0$ and $A_0/A_2 = 2/3$, one finally obtains

$$\tan\beta_2 = \frac{2}{3}\frac{1}{\lambda}\frac{1}{2\left(\sqrt{1+\frac{4}{9\lambda^2}}-1\right)\frac{R_2}{r}+\frac{r}{R_2}} \tag{46}$$

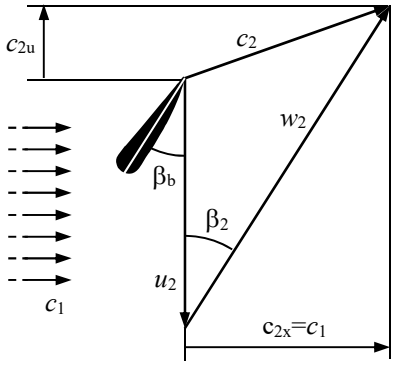

Figure 8. Velocity triangle at the trailing edge of the blade.

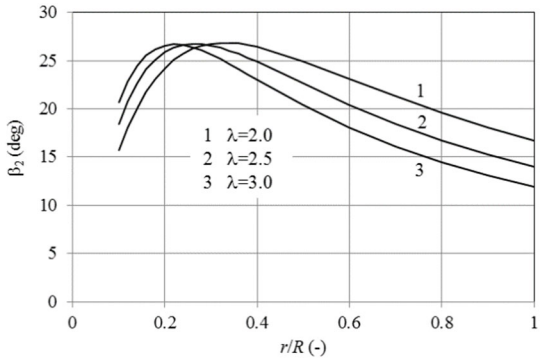

Figure 9. Relative flow angles along the trailing edge of blade for optimum operations at given λ.

Figure 9 shows computation results for three different tip speed ratios. Such flow angles can be basically used as reference to design the blade angles $\beta_b \approx \beta_2$. This, however, relies on the assumption that the flow at the trailing edge of a blade would completely follow the blade angle. This is only the case, if the blade number is sufficiently high. By only using three blades, for instance, the flow angle will deviate from the blade angle. The meaning of all above computations is that corresponding corrections can be made at this final stage of the blade design.

The operation of the wind turbine is specified by the tip speed ratio λ. According to figure 6, the tip speed ratio λ directly determine the power coefficient. On the one hand, a large tip speed ratio should be used. On the other hand, a high tip speed ratio will cause diverse mechanical problems inclusive increased friction losses and operation safety of all related mechanical components. It can be certainly expected that the c_p-curve shown in figure 6 will drop with increased tip speed ratio λ, if viscous friction losses, for instance, are also accounted for. A large tip speed ratio λ always means a large relative velocity (w in figure 8) which, in turn, causes large friction losses on blade surfaces. Because a sufficiently high power coefficient, say 0.57 for a maximum, could be reached already at a tip speed ratio λ=2, there is no need to run the turbine at other high tip speed ratios. This is the reason why wind turbines usually all operate at relatively low rotational speeds.

5. Summary

Diverse flaws or defects in the fundamentals of the wind turbine technology have been pointed out, as they are included in Betz's law and Schmitz's theory. They are considered to be the main cause of contradictions in all previous theoretical analyses.

Against the use of airfoil theory in both flow computations and geometrical designs of turbine blades, the turbine theory of using the Euler equation has been introduced into the wind turbine techniques. Because of the accurate consideration of non-uniform pressure distribution in the flow, the turbine theory and all related computations are accurate. The introduction of the blade efficiency, which is also called the tip swirl number, considerably contributes to the simplification and the completeness of the theoretical analysis. Based on such accurate performance analyses, the reachable maximum power coefficient can be considerably enhanced against the prediction in all previous analyses. With the help of the blade efficiency as a design parameter, the geometrical design of turbine blades has received a significant reference and thus can be well performed.

6. References

[1] Gasch R and Twele J 2012 Wind Power Plants. Second Edition, Springer Verlag.

[2] Sørensen J 2016 General Momentum Theory for Horizontal Axis Wind Turbines, Springer Verlag.